

Stability and crystallization of amorphous clusters in crystalline Si

This article has been downloaded from IOPscience. Please scroll down to see the full text article.

2005 J. Phys.: Condens. Matter 17 4263

(<http://iopscience.iop.org/0953-8984/17/27/003>)

View [the table of contents for this issue](#), or go to the [journal homepage](#) for more

Download details:

IP Address: 129.252.86.83

The article was downloaded on 28/05/2010 at 05:13

Please note that [terms and conditions apply](#).

Stability and crystallization of amorphous clusters in crystalline Si

Sebastian von Alfthan¹, Adrian P Sutton², Antti Kuronen^{1,3} and Kimmo Kaski¹

¹ Helsinki University of Technology, Laboratory of Computational Engineering, PO Box 9203, FIN 02015 HUT, Finland

² Imperial College London, Department of Physics, Exhibition Road, London SW7 2AZ, UK

³ Accelerator Laboratory, University of Helsinki, PO Box 43, FIN-00014, Helsinki, Finland

E-mail: galfthan@lce.hut.fi

Received 17 May 2005, in final form 5 June 2005

Published 24 June 2005

Online at stacks.iop.org/JPhysCM/17/4263

Abstract

We have simulated using molecular dynamics the thermal stability and crystallization kinetics of nanometre-sized clusters of amorphous Si embedded in crystalline Si, which are of interest for phase-change memory devices. We have calculated the interfacial and bulk excess energies of the amorphous clusters, and studied their crystallization kinetics at 700–1500 K. At temperatures below (above) 1150 K the activation energy is 0.73 ± 0.04 eV (1.52 ± 0.07 eV), indicating a change of mechanism at 1150 K. We predict the stability of much larger amorphous clusters by extrapolating our simulation data using an analytic model.

The stability with respect to crystallization of small amorphous clusters embedded in crystals is of both fundamental and technological interest. The creation of amorphous clusters, and their elimination through crystallization, is the basis of phase-change memory devices such as rewritable compact discs [1]. The principal requirements of the technology are the stability of the amorphous clusters against crystallization at ambient temperatures, and an understanding of the kinetics of crystallization as a function of temperature and cluster size. At the fundamental level the kinetics of crystallization of embedded amorphous clusters involves a determination of the activation energy for migration of the interface surrounding the cluster. In this report we present molecular dynamics simulations of the crystallization of amorphous clusters of Si embedded in crystalline Si. Although Si is *not* one of the materials used for phase-change memory devices we have selected it because the availability of reasonable interatomic potentials for Si enables us *to develop a methodology* for investigating the processes involved in these devices. In particular we show how molecular dynamics simulations of the crystallization of relatively small clusters may be used to generate data that can be inserted into an analytic model

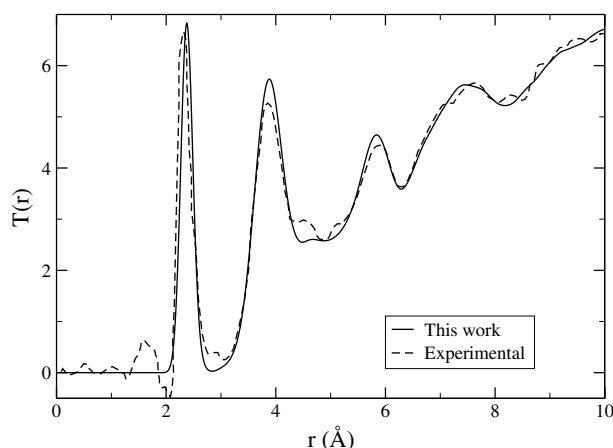


Figure 1. Radial distribution function $T(r) = 4\pi r\rho(r)$ for our simulated amorphous Si sample (solid line) compared to experiment (broken line) [7]. $\rho(r)$ is the average number density of atoms at a distance r from an atom. Our number density has been scaled to the experimental density of $0.054 \text{ atoms } \text{\AA}^{-3}$ and $T(r)$ has been convoluted with a Gaussian with $\sigma = 0.095 \text{ \AA}$.

to predict lifetimes of much larger clusters as a function of temperature. In this way molecular dynamics simulations may be used to make predictions about the stability and lifetimes of realistic cluster sizes, which would otherwise be far too large to model atomistically. The larger clusters have a typical radius of the order of 100 nm while the radius of our simulated clusters is of the order of 2 nm.

In a phase-change memory device a laser beam is used to amorphize an approximately spherical cluster of order 100 nm diameter beneath the surface of a crystalline semiconducting layer. Since the cluster is surrounded by crystal any change of shape undergone by the region that amorphizes has to be accommodated by the crystal. The total number of atoms in the cluster and surrounding crystal is conserved. To model such an embedded amorphous cluster we use a slightly modified version of the procedure introduced by Eshelby [2]. We cut out and remove an approximately spherical 4–6 nm cluster of the perfect crystal, leaving behind a hole. We cut out and remove an approximately spherical cluster of an entirely amorphous sample containing the same number of atoms as the crystallite. If instead we had created an amorphous cluster by melting and quenching the removed crystallite, or by melting and quenching a spherical region of the perfect crystal, the structure of the cluster would have been strongly influenced by its small size as compared with the size of a cluster in a real device. There must be as many atoms in the amorphous cluster as in the removed crystallite to conserve the total number of atoms. However, the volume of the amorphous cluster is larger than the hole in the crystal and it is necessary to compress the cluster by 8% to avoid overlapping material. Once the compressed amorphous cluster has been inserted into the hole in the crystal the whole system has to be relaxed to allow both the interfacial structure and the strain distribution in the cluster and surrounding crystal to be optimized. We carried out this procedure using periodic boundary conditions with one embedded amorphous cluster in each supercell. There was sufficient crystal between the amorphous cluster and its periodic images that their interfacial structures were unaffected by each other.

Bulk amorphous samples were created by quenching a periodically repeated 8000-atom liquid supercell at zero pressure at a rate of 250 K ns^{-1} . The resulting amorphous Si is of very high quality (see figure 1) with a density of $0.0485 \text{ atoms } \text{\AA}^{-3}$. The equations of motion

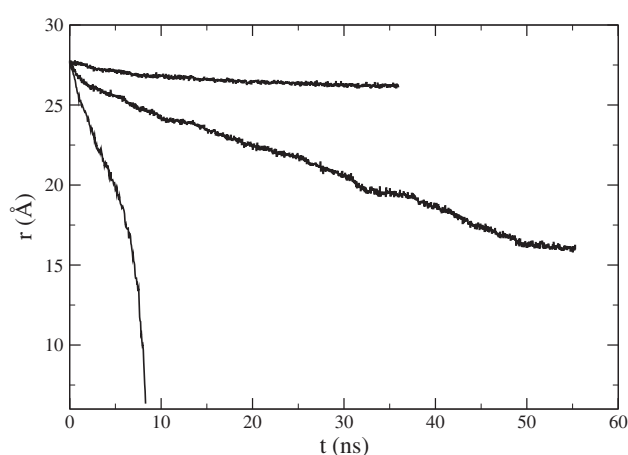


Figure 2. The cluster radius plotted as a function of time for simulations at three different temperatures. The upper curve corresponds to 950 K, the middle curve to 1150 K and the lower curve to 1350 K.

were integrated using the Gear fifth-order predictor–corrector algorithm [3] with a time step of 1 fs. The temperature and pressure were controlled by a Berendsen thermostat [4] and atomic interactions were modelled using the Tersoff III potential [5]. The experimental melting point of Si is 1414 K, and the value computed for the Tersoff III potential is approximately 2550 K [6]. Consequently the simulation temperatures reported below are not on the Kelvin scale but are specific to the potential model.

A spherical cluster of between 3000 and 6000 atoms was cut out of the homogeneous amorphous sample and inserted into a crystalline Si supercell of 21 952 atoms where a spherical hole had been created. By displacing the centre of the spherical cluster by up to 5 Å in the x , y or z direction we were able to generate different initial configurations for the amorphous region and the interface. To relax the entire system we carried out a molecular dynamics simulation with a temperature of 1000 K at a constant supercell volume of $76.02 \times 76.02 \times 76.02 \text{ \AA}^3$ for 3 ns followed by a quench to 0 K at a rate of 500 K ns^{-1} . This relaxation is essential to avoid overestimating the driving force and hence the rate of crystallization. During the relaxation the energy of the system initially fell rapidly, as the interfacial structure and strain distribution throughout the entire system were equilibrated. The total energy then decreased much more slowly as the cluster began to crystallize. During this procedure the radius of the amorphous cluster shrank typically by 1–2 Å and the cluster remained approximately spherical, as seen in figure 3, although pronounced facets parallel to $\{111\}$ were formed. Following this relaxation long molecular dynamics runs were undertaken to allow the cluster to crystallize fully. The molecular dynamics runs simulated up to 50 ns of real time at constant temperatures between 700 and 1500 K using timesteps between 1 and 3 fs. Crystallization of the cluster was effected through the movement of the interface towards the centre of the cluster. In figure 2 the mean spherical radius of a cluster has been plotted as function of time for simulations of the crystallization at three temperatures.

An order parameter that measures the structural disorder of atoms is used to classify atoms as belonging to amorphous or crystalline regions. Thermal disorder is eliminated by calculating the order parameter only for systems quenched to 0 K using conjugate gradient minimization. Atomic positions are compared with atomic sites of a reference Si crystal that extends throughout the supercell and coincides with the crystalline region surrounding the

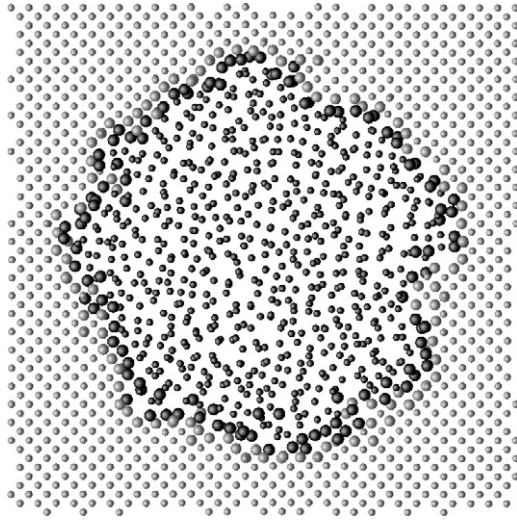


Figure 3. A slice through the system comprising an amorphous cluster of 5000 atoms embedded in crystalline Si, after an initial relaxation. The lighter grey atoms are in the crystalline region, the darker grey in the amorphous region. The location of the interface is indicated by larger atoms.

amorphous cluster. The order parameter p_i for atom i is given by

$$p_i = \Delta r_i - \frac{1}{n_i} \sum_{j \neq i} \Delta r_j, \quad (1)$$

where the summation goes over the n_i atoms within 2.7 \AA of atom i and Δr_i is the smallest distance of atom i from a site of the reference crystal. The second term ensures that a rigid translation in any direction does not change the order parameter. We define the crystalline part of the system to be the largest contiguous cluster of atoms where each atom has a value of p_i less than 0.5 \AA . The rest of the system is then classified as amorphous. In this way atoms within the amorphous region having small values of p_i by chance are correctly classified as belonging to the amorphous cluster.

We calculate the excess internal energy per unit volume of the amorphous cluster, ΔE_v , and the internal energy of the interface per unit area, σ , by approximating the amorphous cluster by a sphere throughout its collapse. To find the mean radius of the cluster we identify the first atomic layers of the amorphous and crystalline regions, respectively. The first amorphous layer consists of all those atoms in the amorphous region which are directly bonded to atoms in the crystalline region and vice versa. The interface is defined to pass between these two layers and the radius of the cluster is calculated as the mean distance of the interface from the centre of the amorphous cluster. In more detail, this is done by calculating the distance of the interface from the centre of the cluster for 10 000 random directions. To calculate the distance to the interface in each direction we first select all atoms within 2 \AA from a line drawn in this direction through the centre of mass of the cluster. The mean distance from the centre of mass (of the furthest atoms identified as members of the cluster and the closest atoms identified as members of the crystal) is defined as the distance to the interface in that direction. Finally, the cluster radius is defined to be the mean value of the distances to the interface for all randomly chosen directions. The excess internal energy of the supercell containing an amorphous cluster compared to a crystalline supercell is then given by

$$E_{xs} = 4/3\pi r^3 \Delta E_v + 4\pi r^2 \sigma. \quad (2)$$

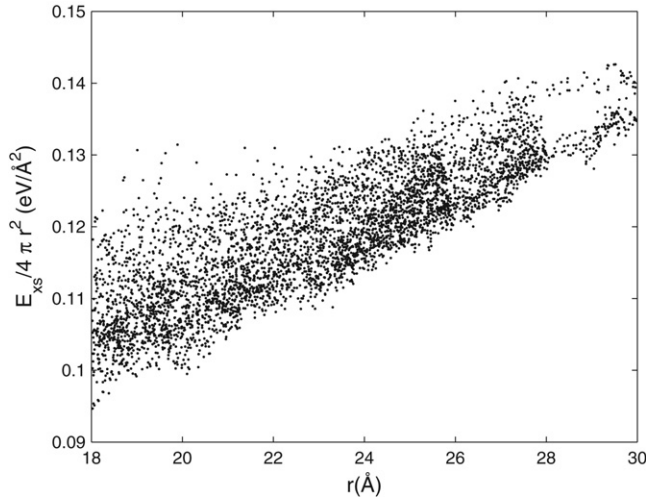


Figure 4. Excess internal energy $E_{xs}/4\pi r^2$ plotted as a function of average radius r of the amorphous cluster.

The excess internal energy was obtained from the supercells, which had been quenched to 0 K, by calculating the excess potential energy of the system compared to a crystalline supercell containing the same total number of atoms. Values of ΔE_v and σ were obtained for each separate simulation of a collapsing cluster, and averaged to yield $\Delta E_v = 1.19 \pm 0.27 \text{ GJ m}^{-3}$ and $\sigma = 1.01 \pm 0.20 \text{ J m}^{-2}$. Alternatively, one can calculate ΔE_v and σ directly from all simulations as follows. In figure 4 we have plotted $E_{xs}/4\pi r^2$ as a function of r . There is a band of points, and in general points on the upper side of the band originate from simulation cells quenched from higher temperatures. This reflects the fact that the interfaces are less ordered at higher temperatures. The low-temperature clusters do not have sufficient time to shrink significantly, and therefore these systems contribute points only at the larger radii. From a straight-line fit to the points we obtain average values of $\Delta E_v = 1.27 \text{ GJ m}^{-3}$ and $\sigma = 0.96 \text{ J m}^{-2}$ for the excess bulk and surface internal energy, respectively. These values are within the uncertainty interval obtained above.

The velocity of the interface is given by

$$\frac{dr}{dt} = \mu \Delta P, \quad (3)$$

where μ is the mobility of the interface and ΔP is the pressure exerted on the interface. The interface mobility follows an Arrhenius-like behaviour. The pressure difference ΔP is given by the negative of the derivative of the excess free energy with respect to volume. ΔP is negative and hence the cluster collapses. We approximate the excess free energy by the excess internal energy. Thus the velocity is given by

$$\frac{dr}{dt} = -v_0 \left(1 + \frac{\rho}{r}\right) \exp\left(-\frac{E}{kT}\right), \quad (4)$$

where E is the activation energy for interface movement, v_0 is a constant and $\rho = 2\sigma/\Delta E_v = 1.7 \text{ \AA}$. Solving equation (4) for r gives

$$r(t) = r(0) - v_0 t \exp\left(-\frac{E}{kT}\right) - \rho \ln\left(\frac{\rho + r(0)}{\rho + r(t)}\right). \quad (5)$$

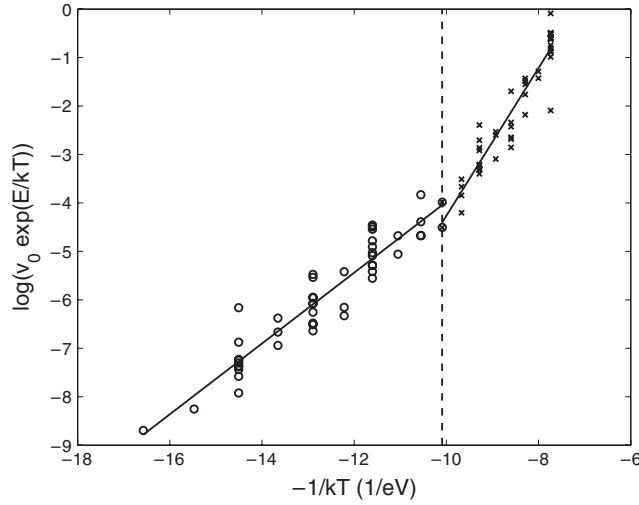


Figure 5. $\ln[v_0 \exp(-E/kT)]$ plotted as a function of $-1/kT$. The dashed line indicates the temperature of 1150 K where the activation energy changes. The two solid lines are straight-line fits to the data points above and below 1150 K.

From the simulations we can extract the radius of the sphere as a function of time. This enables us to deduce the value of $v_0 \exp(-E/kT)$ graphically for each simulation. The logarithmic term on the right is insignificant at r values between 20 and 30 Å where we simulate the collapse. (It is also insignificant in the much larger clusters used in phase-change memory devices.) It follows that the activation energy we obtain below is not sensitive to the calculated values of σ and ΔE_v , and hence to our use of internal rather than free energies for these quantities.

An alternative, but ultimately equivalent, treatment is to use rate theory to write down an equation for the rate at which the number, N_a , of atoms in the amorphous cluster is decreasing through crystallization. In such an approach the rate is proportional to the number of atoms at the surface of the cluster, which scales as $N_a^{2/3}$, because crystallization occurs there. The rate is also proportional to a Boltzmann factor involving the activation energy, E , for migration of the interface. The result is

$$N_a(t)^{1/3} = N_a(0)^{1/3} - ct \exp\left(-\frac{E}{kT}\right) \quad (6)$$

where c is a positive constant. If, as we have argued above, we ignore the logarithmic term on the right-hand side of equation (5) we see that this equation is identical to equation (6) because r is proportional to $N_a^{1/3}$ for a spherical cluster. The advantage of the rate equation approach is that it does not assume a spherical shape for the cluster. In addition, the number of atoms in the cluster is a better defined quantity than its mean radius.

In figure 5 we have plotted $\ln[v_0 \exp(-E/kT)]$ as a function of $-1/kT$. There are two straight-line segments, which intersect at approximately 1150 K. Below 1150 K the activation energy is 0.73 ± 0.04 eV, while above this temperature it is 1.52 ± 0.07 eV. These activation energies are higher than those obtained in [8], where activation energies of 0.23, 0.37 and 0.46 eV were obtained for the *initial* crystallization of amorphous clusters generated by ion beam damage. There are two principal reasons for the lack of agreement between our calculated activation energies and those of [8]. First, the Stillinger–Weber potential [9] for Si was used

in [8], whereas we have used the Tersoff III potential [5]. Second, the quenching rate applied in the creation of the amorphous clusters in [8] was 3–4 orders of magnitude greater than ours, and hence is almost certainly not as relaxed as our configurations. In addition, the simulation times associated with the cluster collapse in [8] were all less than 0.5 ns, 100 times less than in this work. In [10] an activation energy of 0.89 eV was obtained for the migration of interfaces surrounding amorphous clusters of Si, modelled with the same potential as in this work, at simulated temperatures of 1200–1600 K. The activation energy of [10] is lower than the value we obtained above 1150 K. We speculate that this stems from the different ways in which the amorphous clusters were generated and annealed prior to crystallization.

We have carried out detailed structural studies of the interfaces and apparent mechanisms of migration above and below 1150 K to find the reason for the change in activation energy. In particular we have sought to establish whether there is a roughening transition of the interface at 1150 K, below which the interface moves by a ledge mechanism [11] and above which it moves more homogeneously without the creation and motion of localized defects. However, we have not found convincing evidence either for a roughening transition or for a distinct change in mechanism of interfacial motion.

If we assume that the mechanism of migration does not change between 700 K and room temperature, and that it does not change as the cluster size increases to 100 nm, we can calculate the stability of large amorphous clusters at room temperature. Room temperature is the relevant temperature because the key question for a phase-change memory device is the stability against crystallization of the amorphous cluster at ambient temperature. Our assumption that the mechanism of migration does not change as the cluster size increases is justified by the fact that the interface is always sharp and faceted once the cluster size is greater than about 1 nm. It is only at smaller cluster sizes that the interface becomes diffuse, and lateral motion of ledges is replaced by a more uniform motion of the entire interface normal to itself. Similarly there is unlikely to be a change of mechanism of migration as the temperature is *reduced* because it is only at *higher* temperatures that the interface may undergo a roughening transition and bring about a change of mechanism. Taking 0.73 eV for the activation energy, and the prefactor, $v_0 = 27.8 \pm 13.4 \text{ m s}^{-1}$, from our molecular dynamics simulations, we use equation (5) to deduce that the time it takes for a 100 nm spherical cluster to shrink by 10% at 300 K is 11 min. There is an uncertainty in this value of the order of 15 min, which is almost entirely caused by the uncertainty in the activation energy. This is several orders of magnitude smaller than the times required for phase-change memory devices [1], and it indicates that pure Si is not a suitable material. The problem with Si is the low activation energy for the migration of the amorphous–crystalline interface.

It is interesting to compare our results with those of Bording and Taftø [12], who estimated the critical radius of a crystalline nucleus in an amorphous matrix using the Tersoff potential for Ge. They carried out molecular dynamics simulations of spherical crystallites of various sizes embedded in an amorphous matrix with periodic boundary conditions to see whether the crystallites grew or shrank. Once the critical radius of the cluster has been exceeded it will continue to grow and consume the surrounding amorphous matrix. There is a real sense, therefore, in which the phenomenon they simulated is the inverse of that considered in our simulations. They obtained a critical nucleus size of about 2 nm, whereas in our simulations there is no critical size since all amorphous clusters in a crystalline matrix are thermodynamically unstable. There are also significant computational differences: they considered smaller periodic cells (4.5 nm compared with our 7.6 nm), containing fewer atoms (4096 compared with our 21 952), with an equilibration anneal of 10 ps compared with ours of 3 ns, followed by molecular dynamics runs of 0.7 ns compared with our runs of up to 50 ns. These differences reflect the increase of computational power in five years.

In summary, we have carried out a series of molecular dynamics simulations at temperatures between 700 and 1500 K to study the crystallization kinetics of amorphous Si clusters embedded in crystalline Si. Crystallization at temperatures below 700 K may not be studied easily by molecular dynamics owing to the long timescales involved. Similarly, the use of molecular dynamics imposes quite severe limits on the sizes of amorphous clusters that may be completely crystallized in a simulation. But by combining the results of our simulations with a simple analytic model we have been able to predict the crystallization kinetics of larger clusters and at temperatures lower than those accessible by molecular dynamics alone. Our results confirm that Si is not a suitable material for phase-change memory devices because the activation energy for motion of the amorphous–crystalline interface is too low. We have also detected that there is a change of this activation energy at 1150 K.

References

- [1] Ovshinsky S R and Ohta T 2003 *Photo-Induced Metastability in Amorphous Semiconductors* (New York: Wiley–VCH) chapter (Phase-Change Optical Storage Media)
- [2] Eshelby J D 1957 *Proc. R. Soc. A* **241** 376
- [3] Allen M P and Tildesley D J 1989 *Computer Simulation of Liquids* (Oxford: Oxford University Press)
- [4] Berendsen H J C, Postma J P M, van Gunsteren W F, DiNola A and Haak J R 1984 Molecular dynamics with coupling to an external bath *J. Chem. Phys.* **81** 3684–90
- [5] Tersoff J 1988 Empirical interatomic potential for silicon with improved elastic properties *Phys. Rev. B* **38** 9902
- [6] Stephen J 1993 Cook and Paulette Clancy. Comparison of semi-empirical potential functions for silicon and germanium *Phys. Rev. B* **47** 7686
- [7] Kugler S, Molnar G, Petö G, Rosta L, Menelle A and Bellisent R 1989 Neutron-diffraction study of the structure of evaporated amorphous silicon *Phys. Rev. B* **40** 8030
- [8] Caturla M-J, Margués L A, Diaz de la Rubia T and Gilmer G H 1996 Ion-beam processing of silicon at keV energies: A molecular-dynamics study *Phys. Rev. B* **54** 16683
- [9] Stillinger F H and Weber T A 1985 Computer simulation of local order in condensed phases of silicon *Phys. Rev. B* **31** 5262
- [10] Marques L A, Pelaz L, Aboy M, Enriques L and Barbolla J 2003 Microscopic description of the irradiation-induced amorphization in silicon *Phys. Rev. Lett.* **91** 135504
- [11] Sutton A P and Balluffi R W 1995 *Interfaces in Crystalline Materials* (Oxford: Oxford University Press) chapter 9
- [12] Bording J K and Taftø J 2000 Molecular-dynamics simulation of growth of nanocrystals in an amorphous matrix *Phys. Rev. B* **62** 8098